

## Research Paper

# Development of an *in Vitro* Rat Intestine Segmental Perfusion Model to Investigate Permeability and Predict Oral Fraction Absorbed

Marc-Etienne Castella,<sup>1</sup> Marianne Reist,<sup>1</sup> Joachim M. Mayer,<sup>1</sup> Jean-Jacques Turban,<sup>1</sup> Bernard Testa,<sup>2</sup> Claire Boursier-Neyret,<sup>3</sup> Bernard Walther,<sup>3</sup> Jean-Marie Delbos,<sup>3</sup> and Pierre-Alain Carrupt<sup>1,4</sup>

Received May 19, 2005; accepted February 14, 2006

**Purpose.** The aims of the study are to develop and evaluate an *in vitro* rat intestine segmental perfusion model for the prediction of the oral fraction absorbed of compounds and to assess the ability of the model to study intestinal metabolism.

**Methods.** The system consisted of a perfusion cell with a rat intestinal segment and three perfusion circulations (donor, receiver, and rinsing circulation). Lucifer yellow (LY) was applied as internal standard together with test compounds in the donor circulation. To validate the model, the permeability of eight noncongeneric passively absorbed drugs was determined. Intestinal *N*-demethylation of verapamil into norverapamil was followed in the donor and receiver circulations by high-performance liquid chromatography analysis.

**Results.** The *in vitro* model allowed ranking of the tested compounds according to their *in vivo* absorption potential. The Spearman's correlation coefficient between the oral fraction absorbed in humans and the ratio of permeation coefficient of test compound to the permeation coefficient of LY within the same experiment was 0.98 ( $P < 0.01$ ). Moreover, intestinal *N*-demethylation of verapamil, its permeation, and the permeation of its metabolite norverapamil could be assessed in parallel.

**Conclusions.** Up to six permeation kinetics can be obtained per rat, and the method has shown to be a valuable tool to estimate human oral absorption.

**KEY WORDS:** absorption model; *in vitro* intestinal metabolism; *in vitro* intestinal permeability; *in vitro*-*in vivo* correlation; rat jejunal perfusion.

## INTRODUCTION

Developing new chemical entities administered orally and improving their bioavailability are key objectives in drug research. Approaches allowing to evaluate extent, characteristics, and mechanisms of absorption without having to study bioavailability *in vivo* in whole animals are essential to rationally select new viable chemical entities and optimize lead candidates. Various biological models for permeability investigations have been established at different levels of

complexity ranging from intestinal membranes to tissue-based systems and *in situ* intestinal perfusion techniques.

Subcellular fractions and freshly isolated enterocytes are limited to uptake studies rather than to transport studies, and extrapolation to rate and extent of absorption *in vivo* is difficult (1,2). Cell-based assays using human colon adenocarcinoma (Caco-2) or dog kidney (Madin-Darby canine kidney) cell lines are frequently used to estimate drug permeability. In comparison to animal studies, cell-based assays are less expensive, well suited for high-throughput screening, and allow to obtain reproducible permeability values that correlate with intestinal absorption in humans (3–5). On the other hand, cell lines are generally composed solely of absorptive cells and lack mucus, whereas the intestinal epithelium consists of a monolayer of heterogeneous cells including enterocytes, goblet cells secreting mucin, endocrine cells, and M cells. In addition, as the transepithelial electrical resistance is far higher in cell systems than in typical small intestinal tissue, the paracellular permeability is often underestimated. Moreover, the expression of carriers and efflux systems is clearly different in intestinal cell cultures compared to the *in vivo* situation (1,6).

In comparison to simpler models, the presence of apical mucus layer in the tissue-based approaches is an improvement, as it may possibly influence the absorption of compounds. Two different *in vitro* methods relying on

<sup>1</sup>LCT-Pharmacochemistry, School of Pharmaceutical Sciences, EPGL, University of Geneva, University of Lausanne, 30, Quai Ernest Ansermet, CH-1211 Geneva 4, Switzerland.

<sup>2</sup>Département de Pharmacie, Centre Hospitalier Universitaire Vaudois, CH-1011 Lausanne, Switzerland.

<sup>3</sup>Technologie Servier, F-45007 Orléans, France.

<sup>4</sup>To whom correspondence should be addressed. (e-mail: Pierre-Alain.Carrupt@pharm.unige.ch)

**ABBREVIATIONS:**  $F_a$ , oral fraction absorbed; HPLC, high-performance liquid chromatography; LC-MS/MS, liquid chromatography with tandem mass spectrometry;  $\log D_{\text{oct}}^{7.4}$ , octanol water distribution coefficient at pH 7.4;  $\log P^N$ , octanol water partition coefficient of the uncharged species; LY, Lucifer yellow; MW, molecular weight;  $P_{\text{app}}$ , coefficient of apparent permeability;  $P_{\text{eff}}$ , effective permeability coefficients.

isolated tissues have been recurrently used to evaluate drug permeability, measure paracellular transport, and determine regional variability, namely, the everted gut sac technique and the side-by-side Ussing chambers (7–9). In the former method, segments of intestine are turned inside out over a glass rod, tied off at one end, filled with oxygenated buffer, and ligatured at the other end. The resulting sacs are incubated in the presence of test compound for different time periods, and accumulation in the inner compartment is measured. A high tissue viability and integrity was confirmed for up to 120 min when using oxygenated tissue culture medium 199 (7). However, the fluid inside the sac is stagnant, which does not correspond to physiological conditions. In Ussing chambers, the intestine is cut into strips, which are clamped between two glass chambers filled with buffer and nutrients such as glucose. In this setup, the permeation studies can be conducted on intestinal tissue either with or without the underlying muscle layers (10). Because drug absorption into the intestinal vasculature *in vivo* does not involve permeation through the intestinal smooth muscle, the removal of this nonphysiological diffusion barrier—a practice known as stripping—is claimed to be preferable because this resembles more closely the *in vivo* situation (1). A high correlation was reported between the effective permeability coefficients determined in human jejunum *in vivo* and in stripped excised jejunal rat segment in Ussing chambers for a discrete small series of 12 compounds (11). However, the procedure to remove the outer muscle layers from intestinal segments requires extensive expertise in microsurgery and may present a technical barrier to the novice scientist.

Compared to the *in vitro* models described above, *in situ* approaches provide experimental conditions closer to what is encountered following oral administration. *In situ* intestinal perfusion experiments provide an intact blood supply and a functional intestinal barrier. However, these techniques are time and animal consuming and not adapted for high-throughput screening (12).

In summary, as absorption models increase in complexity, an increasing number of factors influencing drug absorption come into play. Unfortunately, the more closely the model approaches the *in vivo* situation, the more it is labor intensive and material and animal consuming (13).

The newly developed *in vitro* rat intestine segmental perfusion model described here is a tissue-based system with perfusion circulations, avoiding stagnant fluid inside the intestinal segment. Up to six experiments per rat can be performed, and less tissue manipulation is required than with Ussing chambers. Because the oral fraction absorbed *in vivo* in rats has been shown to correlate well with that in humans, this rodent was selected as animal model (14,15). Characterization and evaluation of the segmental perfusion model was performed by determining the permeation of eight passively absorbed drugs with a broad range of physicochemical properties and oral fractions absorbed *in vivo*. A good *in vitro*–*in vivo* correlation was obtained, the Spearman's correlation coefficient between the oral fraction absorbed in humans and the ratio of permeation coefficient of test compound to the permeation coefficient of Lucifer yellow (LY) within the same experiment being 0.98 ( $P < 0.01$ ). Finally, preliminary experiments showed the possibility to study metabolism and permeation of drugs and their

metabolites in parallel with the proposed *in vitro* perfusion model. Verapamil and its *N*-demethylated metabolite norverapamil were selected as model compounds, as studies of their absorption and metabolism in rat assessed in Ussing chambers (16–18) and in two *in situ* models (19) are available for comparison (20).

## MATERIALS AND METHODS

### Chemicals

Antipyrine, racemic atenolol, LY CH, mannitol, [2-(*R*), 3-(*S*)]-nadolol, (*S*)-(+)-naproxen, racemic norverapamil, racemic propranolol, sulpiride, testosterone, and racemic verapamil were purchased from Sigma (St. Louis, MO, USA). Polyethylene glycol 4000 (PEG 4000) was obtained from Fluka Biochemica Ultra (Buchs, Switzerland). D-[1-<sup>14</sup>C]Mannitol, [<sup>14</sup>C]PEG 4000, and [4-<sup>14</sup>C]testosterone were acquired from Amersham Pharmacia Biotech (Buckinghamshire, UK). (D,L)-[Ring-<sup>3</sup>H(N)]Atenolol and L-[4-<sup>3</sup>H]propranolol were purchased from NEN Life Science Products (Boston, MA, USA). [3-<sup>14</sup>C]Antipyrine and medium 199 with Earle's salts, L-glutamine, and bicarbonate were obtained from Sigma.

All other chemicals were of analytical grade, and analytical solvents were of high-performance liquid chromatography (HPLC) grade and purity. The Oasis HLB extraction cartridges (10 mg) were supplied by Waters Corporation (Milford, MA, USA).

### Animals and Surgery

Male albino Sprague-Dawley rats (250–400 g) obtained from Charles River Lab (Iffa Credo, L'Arbresle, France) were allowed to acclimatize in our facilities for at least 4 days before sacrifice. They were maintained in cages in an air-conditioned room (21–25°C, 50% humidity) with circadian day/night rhythm of 12 h. Standard rodent chow (No. 950.9, Protector S.A., Lucens, Switzerland) and water were given *ad libitum*. Before the experiment, rats were fasted overnight. The protocol of these studies was approved by the Cantonal Veterinary Service (VD, Switzerland) and was in compliance with the "Principles of Laboratory Animal Care" (NIH publication #85-23, revised 1985). Once euthanized by anoxia with carbonic gas, upon verification of the loss of pain reflex, rats were placed on their back, restrained to the operating platform with adhesive band, and a ventricular longitudinal incision was made from the pubis to just below the diaphragm. Perpendicular incisions at the ends of the longitudinal incision allowed the exposition of the peritoneal cavity. The small intestine was quickly removed, placed in an oxygenated physiological NaCl solution at 37°C, and rinsed with approximately 50 mL oxygenated physiological NaCl solution to remove food particles. The jejunum (segment of 20 cm beginning 30 cm distal to the pylorus) was used for perfusion experiments (10).

### Description of the *in Vitro* Segmental Perfusion System

The *in vitro* segmental perfusion system consisted of the perfusion cell, three perfusion circulations (donor, receiver,

and rinsing circulation including peristaltic pumps and thermostated reservoirs with oxygenation), two bubble traps, an oven, and four three-way stopcocks (see Fig. 1A). The donor medium circulated through the inside of the intestinal segment, while the receiver circulation was flowing outside the intestinal segment, in the opposite direction. The rinsing circulation was needed to facilitate air-bubbles extraction in the segment and to provide a good tissue oxygenation before initiating the experiments. All circulations were thermostated at 37°C, and their oxygenation was assured by bubbling their reservoirs with Carbogen (95% O<sub>2</sub>, 5% CO<sub>2</sub>) under magnetic stirring. The flow rates were established by means of an Ismatec VC-MS/CA peristaltic pump (Ismatec, Zurich, Switzerland) for the rinsing circulation (pump 1), a Masterflex® PTFE-tubing pump (Cole-Parmer Instrument Company, Vernon Hills, IL, USA) for the donor circulation (pump 2), and an LC T-414 pump (Kontron

Instruments, Zurich-Müllingen, Switzerland) for the receiver circulation (pump 3).

The present studies were performed on two identical systems, allowing two kinetics to be carried out in parallel.

**Preparation of Segments**

The central element of the segmental perfusion system consisted of two hollow cylindrical ends connected with concave junctions and allowing the head of one central element to fit into the back of another (Fig. 2). Both hollow cylindrical ends (diameter 0.4 cm) presented a groove. A cap was placed on the head to facilitate introduction in the jejunum.

Avoiding areas containing Peyers patches, both ends of the segments were ligated on the grooves using silk suture. The so-obtained intestinal segments were kept in oxygenated

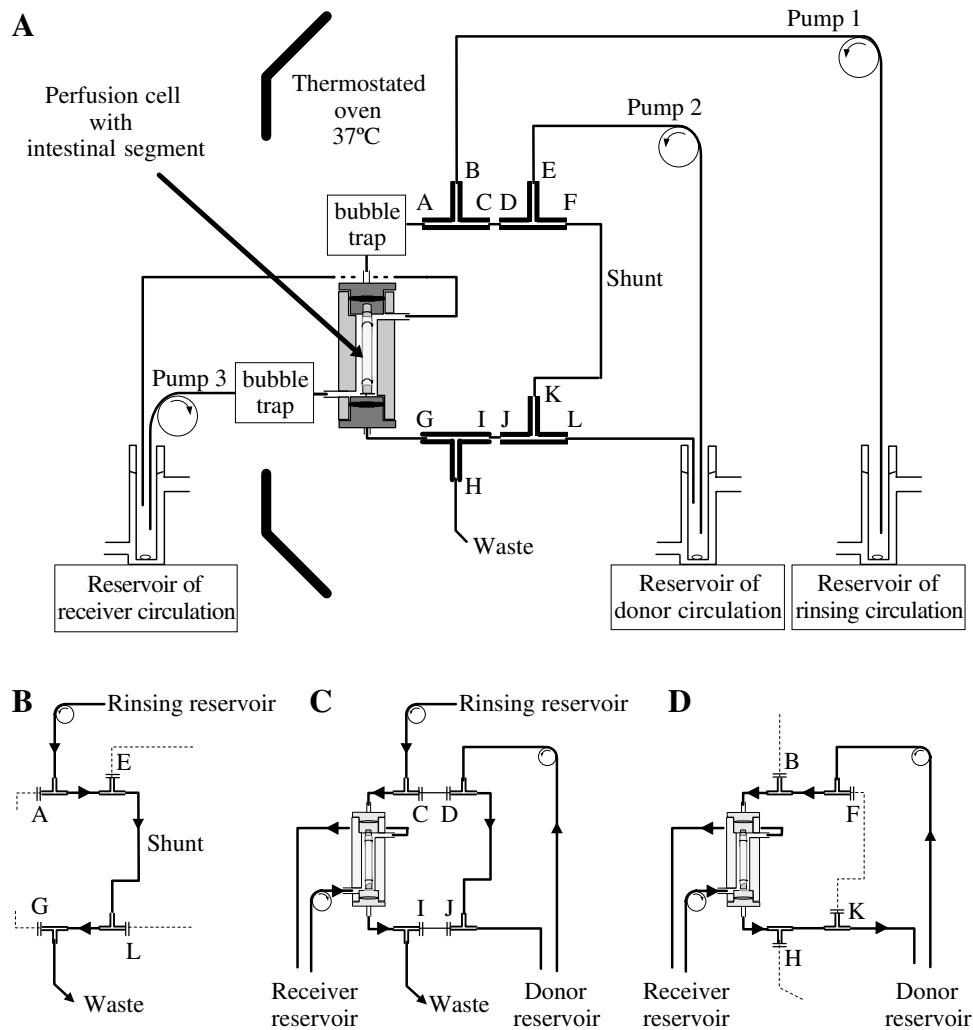


**Fig. 1.** Schematic of the *in vitro* rat intestine segmental perfusion system with its permeation cell, shunt, bubble traps, oven, and three perfusion circulations (A). Before the installation of the permeation cell, the four three-way stopcocks are oriented to block issues A, E, G, and L, while only rinsing circulation's pump 1 is working (B). After the installation of the permeation cell, issues C, D, I, and J are blocked, while the three pumps are switched on (C). Finally, during the permeation kinetic, issues B, F, J, and K are blocked and pump 1 is stopped, so that the oxygenated donor circulation flows without air bubbles inside the segment, whereas the receiver circulation flows outside the segment in the opposite direction (D).

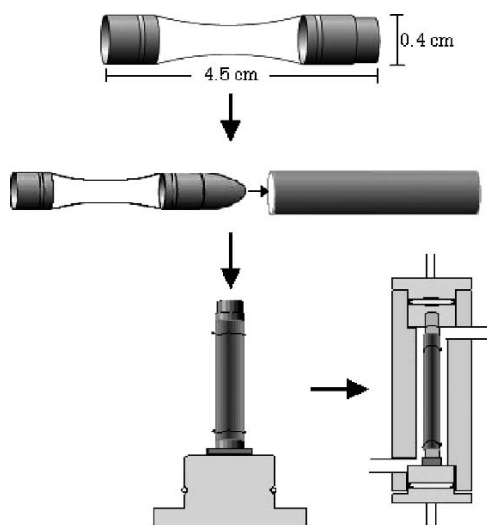


Fig. 2. Preparation of tissue segments.

physiological solution, installed on the bottom part of the perfusion cell, and cap-removed (Fig. 2). Then, the perfusion cells were assembled, and the segments were rinsed with 3 mL of oxygenated medium before being inserted in the perfusion systems.

#### ***In Vitro* Permeation Experiments with the Perfused Segment**

The reservoirs of the receiver and rinsing circulations were filled with 15.0 mL of medium 199. In the donor reservoir, 15.0 mL of medium 199 containing the test compound and LY as internal standard, each at a concentration of 100  $\mu\text{M}$ , was inserted (Fig. 1A). The proportion of radiolabeled test compound was calculated to reach 200,000 dpm/mL in the donor solution.

Three different flow rates (0.2, 0.4, and 0.6 mL/min) were tested for both the rinsing and donor circulations to study the influence of this parameter on the permeation kinetics. During the installation of the perfusion cell into the perfusion system, the three-way stopcocks were oriented to block issues A, E, G, and L (Fig. 1B), permitting circulation of oxygenated medium 199 from the rinsing reservoir to waste via a shunt. Peristaltic pump 1 was set to the selected flow rate.

After installation of the perfusion cell, the orientation of the three-way stopcocks was modified to block issues C, D, I, and J. Consequently, the oxygenated rinsing solution circulated in the segment at the selected flow rate (Fig. 1C). During that time, pump 3 was switched on to allow the receiver circulation to pass outside the segment at 3.0 mL/min. In addition, the donor circulation was homogenized with the medium remaining from the shunt at a high flow rate (5 mL/min) by switching on pump 2.

After extraction of potential air bubbles in the segment using a syringe on the upper bubble trap, the tissue was allowed to equilibrate for 10 min to facilitate reestablishment of ion transport and ensure a good homogenization in the donor circulation.

After this equilibration time, about 45 min after euthanasia of the animal, 150  $\mu\text{L}$  of sample was withdrawn from the donor reservoir to measure initial LY and test

compound concentrations. Pump 1 was switched off, and the flow rate of pump 2 was set to the experimental condition (0.2, 0.4, or 0.6 mL/min). The three-way stopcocks were oriented to close the issues B, F, H, and K, allowing the donor fluid to go through the intestinal segment (time  $t_0$ , see Fig. 1D). The pH values of the donor and receiver solutions were measured before and after the experiments. During approximately 2 h of permeation study, samples (150  $\mu\text{L}$  for compound and LY analysis) were removed every 10–15 min from the receiver circulation and replaced with the same volume of medium.

#### **Evaluation of *in Vitro* Metabolism and Permeation of Verapamil**

To evaluate the chemical stability of verapamil and norverapamil and their possible adsorption onto the perfusion system, 1  $\mu\text{M}$  solutions of these compounds were prepared in medium 199 and circulated in the receiver circulation at 37°C for 3 h with a piece of stainless steel in place of the intestinal segment.

Animal surgery and preparation of the segments were performed as described above. The flow rate was set at 3 mL/min in the receiver circulation and at 0.4 mL/min in the other circulations. The permeation kinetics of parent verapamil and LY—both at an initial donor concentration of 100  $\mu\text{M}$ —were monitored in the donor and receiver circulations for verapamil and in the receiver circulation for LY. The appearance of the metabolite norverapamil as a function of time was investigated in both circulations. Because the flow rate in the donor circulation was low, resulting in poor homogenization, samples from this circulation were taken after the perfusion cell, just before the return into the donor reservoir (see Fig. 1A). The time course of the metabolism experiments was extended to 150 min, and samples were removed every 10 min, alternatively from the donor and receiver circulations. The volume removed (200  $\mu\text{L}$ ) was replaced with an identical volume of medium 199 only in the receiver circulation.

#### **Analytical Methods**

Lucifer yellow and naproxen were assayed alone or together by HPLC on a liquid chromatograph Waters 2690 Separation module (Waters, Millipore) equipped with a Perkin-Elmer LC240 fluorescence detector (Perkin-Elmer, Beaconsfield, UK). The excitation and emission wavelengths were respectively set to 420 and 520 nm for LY and to 270 and 360 nm for naproxen. The HPLC column was a LiChrospher 100 RP-18e (125  $\times$  4 mm i.d., 5  $\mu\text{m}$ ). The isocratic mobile phase consisted of 85% v/v phosphate buffer pH 7.0 and 15% v/v acetonitrile. Calibration curves were calculated to determine concentrations. There was no interference from the medium, tissue-related substances, or tested compounds.

Norverapamil and verapamil were assayed on the HPLC system described above, according to a published method (16). The samples were injected onto an Xterra MS C<sub>18</sub> column (150  $\times$  3.9 mm i.d., 5  $\mu\text{m}$ ) and detected by fluorescence with excitation and emission wavelengths set to 280 and 310 nm, respectively. Baseline separation of

norverapamil from verapamil was complete in the calibration range from 0.02 to 1  $\mu\text{M}$  of norverapamil, independently of the verapamil concentration (0.02–150  $\mu\text{M}$ ). Standard curves for verapamil were established from 0.02 to 150  $\mu\text{M}$ .

The amount of radioactive test compounds in the receiver or donor solutions was monitored using Ultima Gold™ scintillation cocktail from Packard (Pangbourne, UK) and a Packard liquid scintillation counter.

Nadolol was isolated from samples by solid-phase extraction and assayed by liquid chromatography coupled to mass spectrometry using electrospray ionization (LC-MS/MS). Specifically, 200- $\mu\text{L}$  samples diluted ten times and 20.0  $\mu\text{L}$  of sulphiride used as internal standard (stock solution, 200 nM) were extracted from an automated solid-phase extraction system using Oasis cartridges previously solvated with methanol (350  $\mu\text{L}$ ) and purified water (350  $\mu\text{L}$ ). After washing with 500  $\mu\text{L}$  purified water, nadolol and sulphiride were eluted with 150  $\mu\text{L}$  methanol twice and evaporated to dryness under nitrogen at 37°C. The dry extracts were reconstituted with 200  $\mu\text{L}$  of the isocratic mobile phase (50% v/v ammonium formate 20 mM and 50% v/v 0.05% formic acid/acetonitrile). A Quattro LC mass spectrometer (Micromass, Manchester, UK) equipped with an electrospray ionization interface in positive mode with multiple reaction monitoring and Masslynx V 3.4 system software was used for detection. The HPLC system consisted of an Alpha MOS CTC injector maintained at 10°C (Alpha MOS, Toulouse, France) interfaced to a separation module Agilent 1100 series (Agilent Technologies, Palo Alto, CA, USA). A Hy Purity C<sub>18</sub> (10  $\times$  2.1 mm i.d., 5  $\mu\text{m}$ ) guard column and a Hy Purity C<sub>18</sub> (150  $\times$  3.0 mm i.d., 5  $\mu\text{m}$ ) column were used for the chromatographic separations. The isocratic mobile phase was set at a flow rate of 0.2 mL/min, and the tuning parameters were optimized to yield best sensitivity. The calibration range was from 2.5 nM to 2  $\mu\text{M}$ .

### Calculations

The apparent permeability coefficient ( $P_{\text{app}}$ ) of each drug was calculated according to Eq. (1), where  $dQ/dt$  is the steady-state appearance rate in the receiver circulation,  $r$  is the radius of the intestinal tract (0.2 cm),  $L$  is the exposed length of tissue (3 cm), and  $C_0$  is the initial concentration of drug in the donor circulation.

$$P_{\text{app}} = \frac{dQ}{dt} \frac{1}{2\pi r L C_0} \quad (\text{cm/s}) \quad (1)$$

$LY$  was used as internal standard in all experiments, and the results were expressed as the ratio of the  $P_{\text{app}}$  of test compound to the  $P_{\text{app}}$  of  $LY$  determined in the same experiment ( $P_{\text{app}}/P_{\text{app}} LY$ ).

Spearman's rank correlation coefficient ( $r_s$ ), used as a measure of linear relationship between two sets of ranked data, was calculated with Prism 4.0 software (Graphpad, San Diego, CA, USA) according to Eq. (2), where  $d$  is the difference of the two ranks associated with each compound and  $n$  is the number of compounds.

$$r_s = 1 - \frac{6\sum d^2}{(n^3 - n)} \quad (2)$$

## RESULTS

### Development of the *in Vitro* Rat Intestine Segmental Perfusion Model

The development of the *in vitro* rat intestine segmental perfusion model involved the consideration and optimization of various factors, among others adsorption phenomena onto the materials used, tissue viability, flow rates of the perfusion circulations, choice of an internal standard, and reproducibility of the results.

Preliminary experiments showed that testosterone was highly adsorbed onto tubing of Silicone > Tygon® >> Norprene® >> Viton®. In contrast, no binding was observed (after 2 days at room temperature) onto Teflon® or Plexiglas®. Therefore, Teflon® tubing was chosen for the whole system including the peristaltic pumps. The central element was built of stainless steel, and the perfusion cells were made of Plexiglas®. No adsorption of any of the investigated compounds onto these materials was observed.

The flow rate of the receiver circulation was set to 3 mL/min, which was the lowest rate resulting in sufficient homogenization of the receiver circulation and allowing representative samples to be taken every 10–15 min (data not shown). The flow rate of the donor circulation was varied between 0.2 and 0.6 mL/min. For flow rates of 0.2 and 0.4 mL/min, reliable and reproducible results were obtained (Table I). When increasing the gastrointestinal donor flux to 0.6 mL/min, altered nonlinear permeability of the internal standard  $LY$  and the tested compound occurred frequently (data not shown). A donor circulation flow rate between 0.2 and 0.4 mL/min was therefore chosen in all further experiments.

As illustrated in Fig. 3 with two representative permeation studies, the kinetics of permeation and the  $P_{\text{app}}$  of the tested compounds varied considerably between experiments. However, the ratio of the  $P_{\text{app}}$  of test compound to the  $P_{\text{app}}$  of the internal standard  $LY$  in the same experiment was highly reproducible (Table I). Indeed, the example of mannitol (Fig. 3) shows that at a donor circulation flow rate of 0.4 mL/min, the  $P_{\text{app}}$  of mannitol and  $LY$  were 29 and 15 ( $\times 10^{-6}$  cm/s) for rat A and 17 and 9 ( $\times 10^{-6}$  cm/s) for rat B, respectively, whereas the ratios between the  $P_{\text{app}}$  of mannitol and  $LY$  were 1.9 in both experiments. These results clearly show that an internal standard is essential to obtain reproducible results.

**Table I.** Influence of the Flow Rate in the Donor Circulation on the Ratios of the  $P_{\text{app}}$  of Test Compounds to the  $P_{\text{app}}$  of  $LY$  in the Same Experiment

Compound	Donor circulation flow rate			
	0.2 mL/min		0.4 mL/min	
	Ratio <sup>a</sup>	<i>n</i>	Ratio <sup>a</sup>	<i>n</i>
Antipyrine	3.6 $\pm$ 0.1	3	3.7 $\pm$ 0.1	3
Naproxen	2.6 $\pm$ 0.2	3	2.6 $\pm$ 0.3	10
Mannitol	2.2	1	1.9 $\pm$ 0.2	3
Atenolol	1.2	1	1.1 $\pm$ 0.1	4

<sup>a</sup> Mean  $\pm$  standard deviation.

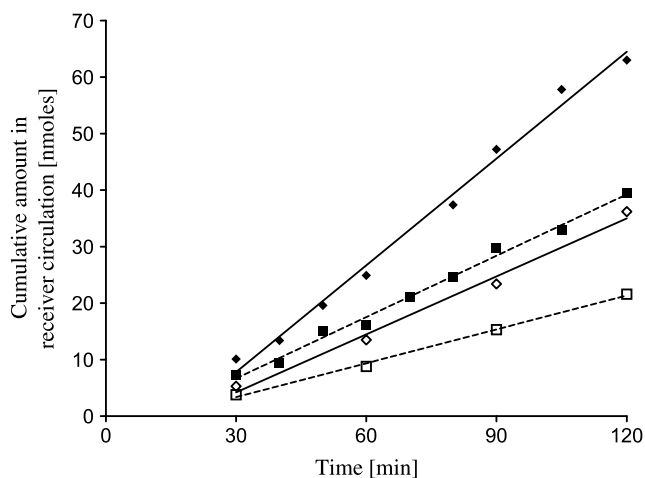


**Fig. 3.** Representative permeation kinetics of mannitol (◆, rat A; ■, rat B) using Lucifer yellow (*LY*) as internal standard (◇, rat A; □, rat B) with a flow rate of 0.4 mL/min in the donor circulation. The  $P_{app}$  of mannitol was different between the experiments, but the ratio to the internal standard was the same.

*LY* is an internal standard with intermediate intestinal permeability (Table II). To evaluate the benefit of a second reference compound with high intestinal permeability, naproxen was inserted in the donor circulation together with *LY*

and test compound (each at 100  $\mu$ M). The permeability of all compounds at a donor circulation flow rate of 0.4 mL/min was determined at least once with both *LY* and naproxen as internal standards. The presence of naproxen had no influence on the ratios between the  $P_{app}$  of the tested compounds and the  $P_{app}$  of *LY*. Because the ratio of the  $P_{app}$  of the two internal standards tested, i.e., naproxen to *LY*, was the same within experimental errors (Table I), the use of a second internal standard was not considered necessary. *LY* was chosen as reference compound in all further experiments.

The pH measured in the oxygenated reservoirs at 37°C was always between 7.2 and 7.4 during the whole experimental procedure. The highest concentration in the receiver circulation at the end of the 2-h perfusion was at most 10% of the initial concentration in the donor circulation.

### Permeation Studies

The *in vitro* rat intestine segmental perfusion model was validated by comparing apparent permeability ratios ( $P_{app}/P_{app, LY}$ ) of eight compounds with the fraction of dose absorbed in man ( $F_a$ ). The ratios of the  $P_{app}$  of test compound to the  $P_{app}$  of *LY* in the same experiment (donor flow rates of 0.2 or 0.4 mL/min inside the segment) are presented in Table II together with literature  $F_a$  values and some physicochemical properties important for permeability

**Table II.** Physicochemical Properties, Oral Fraction Absorbed ( $F_a$ ), and Apparent Permeability Ratios Determined with the *in Vitro* Rat Intestine Segmental Perfusion Model ( $P_{app}/P_{app, LY}$ ), Together with Literature Permeability Values in Ussing Chambers ( $P_{app}$ ) and *in Situ* Perfusion ( $P_{eff}$ )

Compound	MW	$pK_a^a$	$\log P^{Na}$	$\log D_{oct}^{7.4, b}$	$F_a$ <i>in vivo</i> in humans (%)	Ratio $P_{app}/P_{app, LY} \pm SD$ (nb jejunal segments)	Ussing chambers (jejunum), $P_{app} \pm SD$ ( $10^{-6}$ cm/s) <sup>c</sup>	Single-pass intestinal perfusion (ileum), $P_{eff} \pm SD$ ( $10^{-6}$ cm/s) <sup>d</sup>
Testosterone	288	–	3.32	3.32	100 <sup>e</sup>	$5.9 \pm 0.2$ (3)	n.i.	$50 \pm 15^f$
Antipyrine	188	1.44	0.56	0.34	$97 \pm 5^g$	$3.7 \pm 0.1$ (6)	$40 \pm 7$	$73 \pm 2$
Naproxen	230	$4.18^h$	$3.06^h$	0.23	99 <sup>i</sup>	$2.6 \pm 0.3$ (13)	39–51	$167 \pm 82$
Propranolol	259	$9.53^j$	$3.48^j$	1.26	$90^k$ –100 <sup>l</sup>	$2.5 \pm 0.1$ (3)	$29 \pm 2$	$66 \pm 29$
Mannitol	182	–	–3.10	–3.10	65 <sup>m</sup>	$1.9 \pm 0.2$ (4)	$5.9 \pm 2.3$	$7 \pm 5^g$
Atenolol	266	$9.54^j$	$0.22^j$	–1.29	37–71 <sup>n</sup>	$1.1 \pm 0.1$ (6)	$6.0 \pm 0.3$	$18 \pm 9$
Lucifer yellow	457	n.i.	–	–	n.i.	1	n.i.	n.i.
Nadolol	309	9.67	0.71	0.68	$20 \pm 2^o$	$0.7 \pm 0.2$ (3)	n.i.	$4.3 \pm 0.7$
PEG 4000	4000	–	–	–	0 <sup>m</sup>	0 (2)	0 <sup>p</sup>	0 <sup>p</sup>

The  $P_{eff}$  in single-pass perfusion were all taken from references using segments of ileum, luminal pH 7.4 solutions, and 0.2-mL/min flow rate. n.i.: no information available.

<sup>a</sup>  $\log P$  and  $pK_a$  from the MedChem 95 database.

<sup>b</sup> Data from (39) except for testosterone and mannitol, where  $\log D = \log P$ .

<sup>c</sup> Data obtained from (9,11), the pH of the donor and receiver solutions being 7.4.

<sup>d</sup> Data from (12).

<sup>e</sup> Data from (40).

<sup>f</sup> Data from (41).

<sup>g</sup> Data from (42).

<sup>h</sup> Data from (43).

<sup>i</sup> Data from (14).

<sup>j</sup> Data from (44).

<sup>k</sup> Data from (5).

<sup>l</sup> Data from (45).

<sup>m</sup> Data from (22). Note that the value reported for mannitol absorption is higher than other values reported in the literature. Some of this discrepancy may be caused by the apparent hepatic metabolism of mannitol to  $CO_2$ , which is not accounted for in some studies (46). The higher value is consistent with the current data and also with previous published results (22).

<sup>n</sup> Data from (47).

<sup>o</sup> Data from (48).

<sup>p</sup> Data from (21).

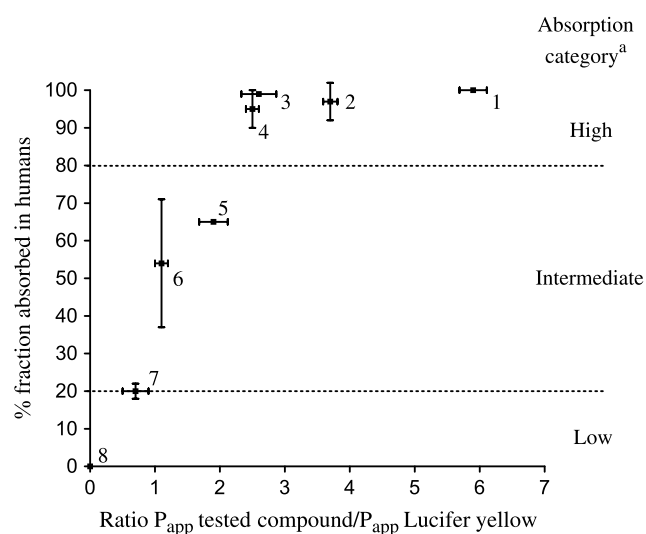


**Fig. 4.** Plot of the ratio of the rat jejunal permeability coefficient of compounds to the permeability coefficient of LY in the same tissue against oral fraction absorbed in humans. Compounds: (1) testosterone, (2) antipyrine, (3) naproxen, (4) propranolol, (5) mannitol, (6) atenolol, (7) nadolol, and (8) PEG 4000. <sup>a</sup>Classification according to (25) and (26).

prediction. The permeability coefficients obtained for the same compounds in Ussing chambers and in single-pass intestinal perfusion are also reported in Table II to compare the predictive value for intestinal absorption of the developed method with the one of these techniques. In Ussing chambers, the coefficients of permeation are based on the appearance of the compound in the receiver compartment ( $P_{app}$ ), whereas in the single-pass intestinal perfusion technique, the effective permeability coefficients ( $P_{eff}$ ) refer to the disappearance of the compound in the lumen.

A plot of the apparent permeability ratios against the oral fraction absorbed in humans is presented in Fig. 4 and shows a good *in vitro*-*in vivo* correlation. Indeed, the *in vitro* rat intestine segmental perfusion model allowed ranking of the tested compounds according to their oral absorption potential in humans with a Spearman's rank correlation coefficient calculated for apparent permeability ratios and oral fractions absorbed in humans of  $0.98$  ( $P < 0.01$ ).

Interestingly, the appearance rate of propranolol in the receiver circulation was nonlinear at the beginning of the experiments, reached steady state around 60 min, and showed a linear time course for the next 60 min. The permeation kinetics of LY in the same experiments were linear from the beginning of the experiment and in a normal range, which confirmed integrity of the tissue. The  $P_{app}$  of propranolol was calculated at steady state, and the ratio between the  $P_{app}$  of propranolol and the one of LY within the same experiment was highly reproducible ( $2.5 \pm 0.1$ ) and consistent with the high oral fraction absorbed *in vivo* (Table II).

### Preliminary Metabolism Studies

The chemical stability of verapamil and norverapamil and their possible adsorption onto the perfusion system was evaluated by circulating 1- $\mu$ M solutions of these compounds in medium 199 in the receiver circulation at 37°C for 3 h with

a piece of stainless steel in place of the intestinal segment. The concentration of both solutions remained constant, and neither degradation nor adsorption was observed.

Preliminary metabolism and permeation experiments of verapamil with the *in vitro* perfusion model showed that verapamil was *N*-demethylated to norverapamil in the jejunal segment. The metabolism as well as the permeation of the parent compound and the metabolite could be followed in parallel, as shown in Fig. 5. Because the permeation of LY was linear and in the same range within the four *in vitro* metabolism/permeation experiments performed, the concentration time profiles of verapamil and its metabolite in the donor circulation at the exit of the perfusion cell (Fig. 5A) and in the receiver circulation (Fig. 5B) were compiled. The net apparent extraction of verapamil from the donor circulation by the intestinal segment remained stable during the time course of the experiment (Fig. 5A). Additionally, an increasing amount of norverapamil was secreted back into the luminal perfusate with respect to time. As was the case with propranolol, a delay was observed before the passage of verapamil into the receiver circulation reached steady state, whereas the passage of LY was linear (Fig. 5B). The ratio of the  $P_{app}$  of parent verapamil calculated at steady state to the  $P_{app}$  of LY in the same experiment was  $2.7 \pm 0.4$  ( $n = 4$ ).

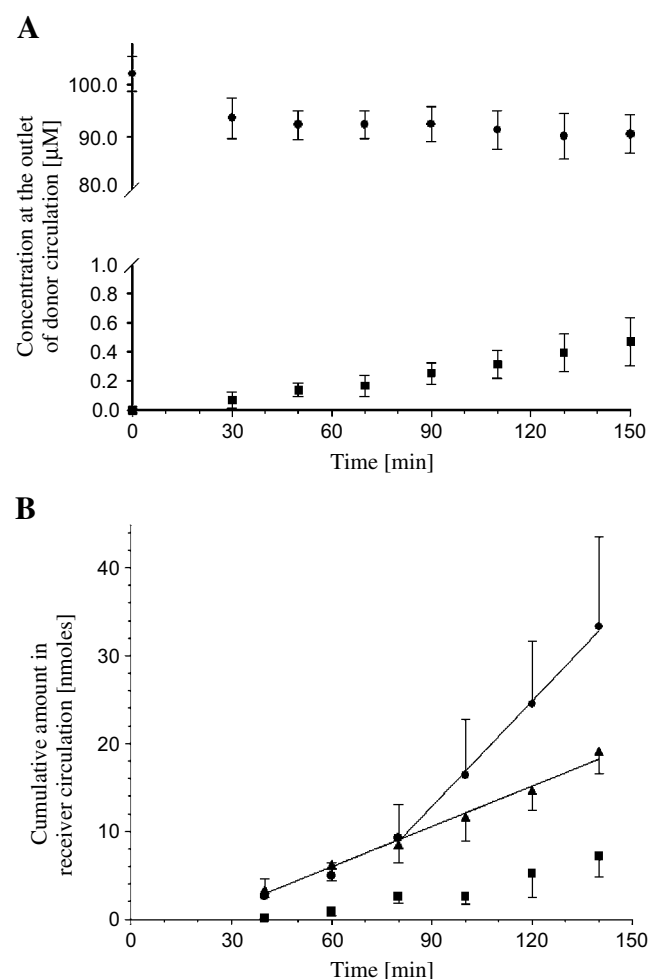


**Fig. 5.** Concentration time profiles of verapamil (●) and formation of norverapamil (■) in presence of LY (▲) at the donor exit of the perfusion cell (A) and in the receiver circulation (B) ( $n = 4$ ).

## DISCUSSION

### Validated Experimental Setup for the *in Vitro* Perfusion Model

A valuable *in vitro* intestinal absorption system should respect the relevant characteristics of the functional intestinal barrier *in vivo* as closely as possible, be reproducible, and be easy to use. Low animal requirement, conservation of a good tissue viability, and prospect for automation would be advantageous. Considering these requirements, an *in vitro* rat intestine segmental perfusion model was developed.

To improve tissue viability, intestinal segments were kept in tissue culture medium 199 (7) and oxygenated with carbogen (95% O<sub>2</sub>, 5% CO<sub>2</sub>).

Experiments performed to optimize the donor circulation flow rate showed that the ratios of the  $P_{app}$  of test compound to the  $P_{app}$  of *LY* in the same experiment were highly reproducible when the donor circulation flux was set to 0.2 or 0.4 mL/min. Furthermore, there was no significant difference between the ratios at both fluxes ( $P < 0.05$ , Table I). However, when this flux was risen to 0.6 mL/min, the kinetics of permeation frequently showed an altered permeability for both tested compound and internal standard, resulting in poor reproducibility of the permeation data. This might be caused by turbulences within the intestinal segment at this higher flow rate, but degradation of the mucus layer or increased physical stress on the cells might be other explanations. A donor circulation flow rate of 0.6 mL/min was therefore considered to be too high. As the cumulated amount seemed slightly higher and the homogenization was supposed to be improved with a flow rate of 0.4 mL/min in comparison to 0.2 mL/min, the experiments were carried out preferentially at this higher flow rate. In addition, no significant regional difference in the  $P_{app}$  values nor in the  $P_{app}$  ratio of test compound to internal standard was observed between the upper and lower parts of the rat jejunum section used in this study.

The use of an internal standard is known to improve the prediction of the oral absorption of drugs (22). With predilection for a nonradioactive internal standard, *LY* was preferred to fluorescein because the latter was reported to present a nonpolarized transport poorly affected by pH via passive paracellular pathways in Caco-2 cells (23). The variability between experiments in coefficients of permeation obtained for the compounds tested was radically reduced when rationalizing with the coefficient of permeation of *LY* in the same experiment (see Fig. 3 and Table I). This variability in the  $P_{app}$  observed between experiments might be explained by small changes of the donor flux, by variations in the tissue surface exposed, or by interanimal variability. Normalizing with the  $P_{app}$  of *LY* obtained under identical experimental conditions than the test compound allowed correcting for these variations. Moreover, *LY* was indicative of tissue integrity and allowed rejection of leaky tissues, which led to nonlinear, increased, and irrelevant kinetics. Indeed, for leaky tissues, the permeation of both *LY* and tested compound were not linear for the duration of the experiment, suggesting that the tissue did not remain intact. In summary, the presence of an internal standard turned out to be essential for the validation of tissue integrity and for a

better relevance of results to predict *in vivo* oral absorption. The use of a second internal standard with a high intestinal permeability, e.g., naproxen, might corroborate the results, but was not considered to be essential because the ratio between the  $P_{app}$  of the two internal standards was constant (Table I).

In the current version of the *in vitro* perfusion model, the volume used in the donor reservoir was rather high (15 mL), which might limit its use to relatively inexpensive compounds that can be used in micromolar concentrations. However, the present prototype might be miniaturized to limit this drawback.

### Permeation Studies

The compounds selected for the validation of the system presented very diverse physicochemical properties and were chosen to cover the whole range of oral fractions absorbed, from 0 to 100%. No values of log  $P$  and  $pK_a$  are indicated for PEG 4000 in Table II, as they are not relevant for a polymer. *LY* is expected to have five  $pK_a$  values below 5 (three acidic and two basic) and to be ionized at neutral pH. Indeed, at pH 7.4, the two weakly basic groups are unionized, whereas the three acidic groups (two sulfates and one N-acidic group) are negatively charged. The stability in phosphate-based buffered solutions at 37°C for 150 min was reported for the majority of compounds tested (16,21). A potential effect because of metabolism on the permeation rates might have influenced the calculation of the permeability coefficients for some of these compounds; however, this was not evaluated further in this study.

As can be seen in Fig. 4, the new *in vitro* perfusion model correctly divided the compounds into low ( $F_a < 20\%$ ), medium ( $F_a = 20 - 80\%$ ), and high ( $F_a > 80\%$ ) absorption drugs, according to an extended version of the biopharmaceutics classification system (24) used by several authors (25,26). Actually, the apparent permeability ratios were predictive for a compound not absorbed at all in humans (PEG 4000), as well as for intermediately absorbed compounds (nadolol, *LY*, atenolol, and mannitol) and highly absorbed drugs (propranolol, naproxen, antipyrine, and testosterone). Most notably, the range of ratios between poorly and highly absorbed drugs (0–2.5) allowed discrimination of intermediately absorbed drugs. Moreover, the lack of absorption of PEG 4000 and its full recovery in the donor circulation at the end of the experiments also assessed the integrity of the intestinal mucosa in the segments. Interestingly, the developed model suggested mannitol to be absorbed at a higher extent than atenolol. This was consistent with the value of fraction absorbed in humans reported in Table II and also with previously published results (22). On the other hand, both in Ussing chambers and in single-pass intestinal perfusion, the extent of permeation of mannitol was similar to the one of atenolol, but with high standard deviations (Table II).

Spearman's rank correlation coefficient between the apparent permeability ratios ( $P_{app}/P_{app, LY}$ ) in the *in vitro* rat intestine segmental perfusion model and oral fraction absorbed in humans was 0.98 ( $P < 0.01$ ), indicating the good predictive power of the model. Comparison with *in situ* single-pass intestinal perfusion and Ussing chambers



strengthens the high predictive quality of the developed model. Indeed, the coefficient of Spearman between the ileal effective permeability *in situ* and the oral fraction absorbed for the same series of compounds was 0.83 ( $P < 0.05$ ).  $P_{\text{eff}}$  values in the ileum were used for comparison, as they were available for all tested compounds under identical perfusion conditions (flow rate at 0.2 mL/min, donor solution of pH 7.4) and as no statistical difference was reported between the  $P_{\text{eff}}$  in the jejunum and the ileum for a discrete series of compounds (22). In Ussing chambers, no information was available on the rat jejunal  $P_{\text{app}}$  of testosterone, nadolol, and LY. Therefore, estimation of Spearman's rank correlation coefficient between  $P_{\text{app}}$  in Ussing chambers and  $F_a$  was not considered relevant for comparison. Nevertheless, ranking of the compounds according to their permeability was similar between rat jejunal segments in Ussing chambers and in the *in vitro* perfusion model (Table II), the pH of donor and receiver medium being 7.4 in both setups.

In the Caco-2 model, the permeation kinetics of propranolol presented a uniform linear passage across the cells without delay and with similar  $P_{\text{app}}$  values, whether calculated with or without metabolites (27). Hence, the delay of 60 min observed to reach an apparent steady-state permeation in the receiver circulation of the *in vitro* segmental perfusion model was unlikely to be explained by the formation of metabolites with different apparition kinetics nor by a potential efflux mechanism or by physiologically relevant binding to components of the enterocytes. In the literature, high accumulation of propranolol within tissue of rat jejunum associated with poor permeability in Ussing chambers during 1 h of experiment has already been reported (28). Because propranolol was shown to present high permeability *in situ* in agreement with the high oral fraction absorbed for this compound, which is between 90 and 100% (Table II), the contradiction with the poor absorption in the tissue-based *in vitro* model was suggested to be the consequence of substantial differences in the passage through the intestinal membrane between the *in vitro* and the *in situ* situations (28). Indeed, in Ussing chambers as well as in the *in vitro* rat intestine segmental perfusion model, once the epithelium has been crossed, a diffusion through the villi—and also eventually through the remaining muscle layers—is necessary to reach the serosal side. These phenomena do not occur *in situ* or *in vivo* where the compound only has to diffuse to the vicinity of capillaries adjacent to the basement membranes of absorptive cells in the lamina propria of the villi (29). This nonphysiological diffusion barrier present in *in vitro* tissue-based systems was suggested to influence the permeation kinetics of cationic lipophilic compounds binding to the villi and muscle layers. Indeed, propranolol and sulfapyridine were shown to be taken up by the jejunal tissue in the side-by-side diffusion chambers model (28). It can thus be assumed that the initial nonlinear time course of propranolol appearance in the receiver solution detected was a result of tissue binding. After 60 min, tissue binding reached saturation, and linear permeation kinetics were observed. This is in agreement with a permeation study during 180 min in Ussing chambers where jejunal segments showed a lower  $P_{\text{app}}$  for propranolol after 60 min than after 120 min (30). Because the calculation of the coefficient of permeation is based on the steady-state passage

of a compound, the appearance rate of test compounds in the receiver circulation was estimated on the linear part of their permeation kinetics, at steady state. Hence, the nonphysiological diffusion barrier present in the *in vitro* rat intestine segmental perfusion model is thought to influence the permeation kinetics of cationic lipophilic compounds but not their permeation coefficients calculated at steady state. Indeed, the ratio of the  $P_{\text{app}}$  of propranolol to the  $P_{\text{app}}$  of LY obtained was reproducible (Table II) and correctly predicted a high  $F_a$  for propranolol (Fig. 4).

### Preliminary Metabolism Studies

Because the small intestine not only acts as an absorptive organ, but also as the first metabolic barrier encountered by orally administered drugs, the ability of the developed *in vitro* rat intestine segmental perfusion model to study both metabolism and permeation in parallel is an asset. Verapamil was selected as model compound because many data were available on its absorption and metabolism in rat jejunum (16–20). Generally, these studies were performed with extracted blood samples or in simple balanced salt solutions, so that other metabolites of verapamil than norverapamil could be detected. In the present preliminary study, these metabolites were not separated from background peaks of components of medium 199, and hence, only metabolism to norverapamil was considered. The enzymes involved in the *N*-demethylation of verapamil are cytochromes  $P_{450}$  3A, which are implicated in the metabolism of more than 50% of the drugs on the market (16,31,32). Because both verapamil and its metabolite norverapamil are known to be actively secreted back in the luminal tract by efflux transporters, the appearance of norverapamil was also investigated in the donor circulation of our setup. Given that the flow rate in the donor circulation was low (0.4 mL/min), sampling in the reservoir would not have been representative of the mean concentration in this circulation. Therefore, the appearance of norverapamil in the donor circulation was monitored after the perfusion cell, just before turning back into the donor reservoir. To be exposed to the cytochromes  $P_{450}$  3A, which are located intracellularly in the mature villous enterocytes (33), verapamil had to enter the cytosol of these cells either once or several times, this drug being substrate of efflux transporters. The increasing amount of norverapamil secreted back into the luminal perfusate with respect to time clearly demonstrated the functionality of the CYP 3A in our setup throughout the 150 min of the experiments, confirming the functionality of the tissue during the time course of the experiments.

In the receiver circulation, as was the case with propranolol, a delay was observed before the passage of verapamil reached steady state, whereas the passage of LY was linear (Fig. 5B). Tissue uptake of verapamil and an apparent increase in the permeation rate of verapamil at a 20- $\mu$ M donor concentration after 60–90 min was also documented in Ussing chambers (16). These observations corroborate the hypothesis that the nonlinear permeation kinetics exhibiting a marked delay before reaching steady state in the *in vitro* rat intestine segmental perfusion model were related to tissue binding. Because the transformation of verapamil into other metabolites than norverapamil was not

taken into account in the apparent permeation kinetics of verapamil and because other supplementary samples were taken from the donor side, the results obtained with this compound were not compiled with the ones presented above for the validation of the method. Nevertheless, the ratio of the  $P_{app}$  of parent verapamil at steady state with an initial donor concentration of 100  $\mu\text{M}$  to the  $P_{app}$  of LY in the same experiments was  $2.7 \pm 0.4$  ( $n = 4$ ), predicting a high absorption of verapamil, which was in good agreement with its oral fraction absorbed of 100% (14).

### Interest of the *in Vitro* Rat Intestine Segmental Perfusion Model

In comparison to *in situ* techniques, the model presented here is less close to the *in vivo* situation. However, up to six segments of jejunum can be taken, and hence, up to six permeation kinetics can be obtained per rat, which contributes to reduce animal consumption. As in the other tissue-based *in vitro* systems, the apical mucus layer is present, which is an advantage, as it may possibly influence the absorption of compounds. Compared to Ussing chambers and everted sacs, less tissue manipulation is required during the preparation of the segments. In contrast to the cell-based systems, the *in vitro* rat intestine segmental perfusion model is not planned for high-throughput screening, but rather as a complementary, user-friendly absorption test for new chemical entities to comfort results obtained with simpler *in vitro* models. The method described here offers the possibility to evaluate the intestinal metabolism of drugs in parallel with permeation studies of parent compounds and metabolites. It is intended to allow a high experimental control (e.g., of compound concentrations, perfusion rates, pH, and coadministration of absorption promoters, efflux, or metabolism inhibitors). With its flexibility, the impact of most experimental factors susceptible to influence the absorption of a compound might be assessed separately, which is likely to contribute to a better understanding of the mechanisms involved in the absorption of a compound and to evaluate metabolism and absorption interactions.

Recently, several attempts to develop models predicting the absorption rate of drugs that take into account solid drug dissolution and pH changes in the gastrointestinal tract have been published (34–38). Using the flexibility of the *in vitro* rat intestine segmental perfusion model, perspectives of this work include the replacement of the donor reservoir by a traditional paddle dissolution chamber or even the installation of a flow-through cell dissolution apparatus with subsequent flow reducers before reaching the perfusion cell. Thus, with few adaptations, the proposed model might evaluate the influence of excipients and formulation on the permeation of poorly water-soluble drugs. Finally, future sample automation is possible.

### CONCLUSION

The developed *in vitro* rat intestine segmental perfusion model has shown to be a valuable tool to estimate oral absorption of compounds in humans. It allowed ranking of the tested compounds according to their oral absorption

potential. Additionally, it was demonstrated that the permeation and metabolism of a drug, as well as permeability characteristics of metabolites formed from the parent compound, can be evaluated in parallel.

### ACKNOWLEDGMENTS

We thank Marie-Paule Le Bon, Josseline Le Gourrierenc, and Jacky Pothier for the analyses of nadolol samples. Also, we are grateful to Catherine Canovi for her advices and skilful technical assistance.

### REFERENCES

1. J. J. Tukker. *In vitro* methods for the assessment of permeability. In J. B. Dressman H. Lennernäs (eds.), *Oral Drug Absorption—Prediction and Assessment Vol. 106*, Marcel Dekker Inc., New York, 1996, pp. 51–72.
2. K. Koga, M. Murakami, and S. Kawashima. Effects of fatty acid sucrose esters on ceftibuten transport by rat intestinal brush-border membrane vesicles. *Biol. Pharm. Bull.* **21**:747–751 (1998).
3. I. J. Hidalgo, T. J. Raub, and R. T. Borchardt. Characterization of the human colon carcinoma cell line (Caco-2) as a model system for intestinal epithelial permeability. *Gastroenterology* **96**:736–749 (1989).
4. P. Artursson and R. T. Borchardt. Intestinal drug absorption and metabolism in cell cultures: Caco-2 and beyond. *Pharm. Res.* **14**:1655–1658 (1997).
5. J. D. Irvine, L. Takahashi, K. Lockhart, J. Cheong, J. W. Tolan, H. E. Selick, and J. R. Grove. MDCK (Madin–Darby canine kidney) cells: a tool for membrane permeability screening. *J. Pharm. Sci.* **88**:28–33 (1999).
6. A. Braun, S. Hämmerle, K. Suda, B. Rothen-Rutishauser, M. Günthert, S. D. Kramer, and H. Wunderli-Allenspach. Cell culture as tools in biopharmacy. *Eur. J. Pharm. Sci.* **11**:S51–S60 (2000).
7. L. Barthe, J. F. Woodley, S. Kenworthy, and G. Houin. An improved everted gut sac as a simple and accurate technique to measure paracellular transport across the small intestine. *Eur. J. Drug Metab. Pharmacokinet.* **23**:313–323 (1998).
8. Z. T. Chowhan and A. A. Amaro. Everted rat intestinal sacs as an *in vitro* model for assessing absorptivity of new drugs. *J. Pharm. Sci.* **66**:1249–1253 (1977).
9. A. L. Ungell, S. Nylander, S. Bergstrand, A. Sjöberg, and H. Lennernäs. Membrane transport of drugs in different regions of the intestinal tract of the rat. *J. Pharm. Sci.* **87**:360–366 (1998).
10. P. L. Smith. Methods for evaluating intestinal permeability and metabolism *in vitro*. In R. T. Borchardt P. L. Smith G. Wilson (eds.), *Models for Assessing Drug Absorption and Metabolism Vol. 8*, Plenum, New York, 1996, pp. 13–34.
11. H. Lennernäs, S. Nylander, and A. L. Ungell. Jejunal permeability: a comparison between the Ussing chamber technique and the single-pass perfusion in humans. *Pharm. Res.* **14**:667–671 (1997).
12. L. Salphati, K. Childers, L. Pan, K. Tsutsui, and L. Takahashi. Evaluation of a single-pass intestinal-perfusion method in rat for the prediction of absorption in man. *J. Pharm. Pharmacol.* **53**:1007–1013 (2001).
13. K. Palm, P. Artursson, and K. Luthman. Experimental and theoretical predictions of intestinal drug absorption. In H. van de Waterbeemd B. Testa G. Folkers (eds.), *Computer-Assisted Lead Finding and Optimization*, Wiley-VCH, Weinheim, 1997, pp. 277–289.
14. Y. H. Zhao, M. H. Abraham, J. Le, A. Hersey, C. N. Luscombe, G. Beck, B. Sherborne, and I. Cooper. Evaluation of rat intestinal absorption data and correlation with human intestinal absorption. *Eur. J. Med. Chem.* **38**:233–243 (2003).
15. G. L. Amidon, P. J. Sinko, and D. Fleisher. Estimating human oral fraction dose absorbed: a correlation using rat intestinal

- membrane permeability for passive and carrier-mediated compounds. *Pharm. Res.* **5**:651–654 (1988).
16. B. M. Johnson, W. N. Charman, and C. J. Porter. Application of compartmental modelling to an examination of *in vitro* intestinal permeability data: assessing the impact of tissue uptake, p-glycoprotein, and CYP3A. *Drug Metab. Dispos.* **31**:1151–1160 (2003).
  17. B. M. Johnson, W. N. Charman, and C. J. Porter. The impact of p-glycoprotein efflux on enterocyte residence time and enterocyte-based metabolism of verapamil. *J. Pharm. Pharmacol.* **53**:1611–1619 (2001).
  18. B. M. Johnson, W. N. Charman, and C. J. Porter. An *in vitro* examination of the impact of polyethylene glycol 400, pluronic P85 and vitamin E D- $\alpha$ -tocopheryl polyethylene glycol 1000 succinate on p-glycoprotein efflux and enterocyte-based metabolism in excised rat intestine. *AAPS Pharm. Sci.* **4**:E40 (2002).
  19. R. Sandstrom and H. Lennernäs. Repeated oral rifampicin decreases the jejunal permeability of R/S-verapamil in rats. *Drug Metab. Dispos.* **27**:951–955 (1999).
  20. B. M. Johnson, W. Chen, R. T. Borchardt, W. N. Charman, and C. J. Porter. A kinetic evaluation of the absorption, efflux, and metabolism of verapamil in the autoperfused rat jejunum. *J. Pharmacol. Exp. Ther.* **305**:151–158 (2002).
  21. U. Fagerholm, M. Johansson, and H. Lennernäs. Comparison between permeability coefficients in rat and human jejunum. *Pharm. Res.* **13**:1336–1342 (1996).
  22. M. E. Dowty and C. R. Dietsch. Improved prediction of *in vivo* peroral absorption from *in vitro* intestinal permeability using an internal standard to control for intra- and inter-rat variability. *Pharm. Res.* **14**:1792–1797 (1997).
  23. Y. Konishi, K. Hagiwara, and M. Shimizu. Transepithelial transport of fluorescein in Caco-2 cell monolayers and use of such transport in *in vitro* evaluation of phenolic acid availability. *Biosci. Biotechnol. Biochem.* **66**:2449–2457 (2002).
  24. G. L. Amidon, H. Lennernäs, V. P. Shah, and J. R. Crison. A theoretical basis for a biopharmaceutic drug classification: the correlation of *in vitro* drug product dissolution and *in vivo* bioavailability. *Pharm. Res.* **12**:413–420 (1995).
  25. S. Winiwarter, N. M. Bonham, F. Ax, A. Hallberg, H. Lennernäs, and A. Karlen. Correlation of human jejunal permeability (*in vivo*) of drugs with experimentally and theoretically derived parameters. A multivariate data analysis approach. *J. Med. Chem.* **41**:4939–4949 (1998).
  26. C. A. Bergström, M. Strafford, L. Lazorova, A. Avdeef, K. Luthman, and P. Artursson. Absorption classification of oral drugs based on molecular surface properties. *J. Med. Chem.* **46**:558–570 (2003).
  27. G. W. Caldwell, S. M. Easlick, J. Gunnet, J. A. Masucci, and K. Demarest. *In vitro* permeability of eight beta-blockers through Caco-2 monolayers utilizing liquid chromatography/electrospray ionization mass spectrometry. *J. Mass Spectrom.* **33**:607–614 (1998).
  28. S. Yamashita, Y. Tanaka, Y. Endoh, Y. Taki, T. Sakane, T. Nadai, and H. Sezaki. Analysis of drug permeation across Caco-2 monolayer: implication for predicting *in vivo* drug absorption. *Pharm. Res.* **14**:486–491 (1997).
  29. J. R. Pappenheimer and C. C. Michel. Role of villus microcirculation in the intestinal absorption of glucose: coupling of epithelial with endothelial transport. *J. Physiol.* **553**:561–574 (2003).
  30. B. I. Polentarutti, A. L. Peterson, A. K. Sjöberg, E. K. Anderberg, L. M. Utter, and A. L. Ungell. Evaluation of viability of excised rat intestinal segments in the Ussing chamber: investigation of morphology, electrical parameters, and permeability characteristics. *Pharm. Res.* **16**:446–454 (1999).
  31. J. Kalitsky-Szirtes, A. Shayeganpour, D. R. Brocks, and M. Piquette-Miller. Suppression of drug-metabolizing enzymes and efflux transporters in the intestine of endotoxin-treated rats. *Drug Metab. Dispos.* **32**:20–27 (2004).
  32. Y. H. Wang, D. R. Jones, and S. D. Hall. Prediction of cytochrome P450 3A inhibition by verapamil enantiomers and their metabolites. *Drug Metab. Dispos.* **32**:259–266 (2004).
  33. J. C. Kolars, P. Schmiedlin-Ren, W. O. Dobbins, J. Schuetz, S. A. Wrighton, and P. B. Watkins. Heterogeneity of cytochrome P450 3A expression in rat gut epithelia. *Gastroenterology* **102**:1186–1198 (1992).
  34. M. J. Ginski and J. E. Polli. Prediction of dissolution–absorption relationships from a dissolution/Caco-2 system. *Int. J. Pharm.* **177**:117–125 (1999).
  35. M. Kobayashi, N. Sada, M. Sugawara, K. Iseki, and K. Miyazaki. Development of a new system for prediction of drug absorption that takes into account drug dissolution and pH change in the gastro-intestinal tract. *Int. J. Pharm.* **221**:87–94 (2001).
  36. X. He, M. Sugawara, M. Kobayashi, Y. Takekuma, and K. Miyazaki. An *in vitro* system for prediction of oral absorption of relatively water-soluble drugs and ester prodrugs. *Int. J. Pharm.* **263**:35–44 (2003).
  37. M. Kataoka, Y. Masaoka, Y. Yamasaki, T. Sakane, H. Sezaki, and S. Yamashita. *In vitro* system to evaluate oral absorption of poorly water-soluble drugs: simultaneous analysis on dissolution and permeation of drugs. *Pharm. Res.* **20**:1674–1680 (2003).
  38. F. Meriani, N. Coceani, C. Sirotti, D. Voinovich, and M. Grassi. *In vitro* nimesulide absorption from different formulations. *J. Pharm. Sci.* **93**:540–552 (2003).
  39. C. Zhu, L. Jiang, T. M. Chen, and K. K. Hwang. A comparative study of artificial membrane permeability assay for high-throughput profiling of drug absorption potential. *Eur. J. Med. Chem.* **37**:399–407 (2002).
  40. P. Artursson and J. Karlsson. Correlation between oral drug absorption in humans and apparent drug permeability coefficients in human intestinal epithelial (Caco-2) cells. *Biochem. Biophys. Res. Commun.* **175**:880–885 (1991).
  41. K. Tsutsumi, S. K. Li, A. H. Ghanem, N. F. Ho, and W. I. Higuchi. A systematic examination of the *in vitro* Ussing chamber and the *in situ* single-pass perfusion model systems in rat ileum permeation of model solutes. *J. Pharm. Sci.* **92**:344–359 (2003).
  42. M. Eichelbaum, H. R. Ochs, G. Roberts, and A. Somogyi. Pharmacokinetics and metabolism of antipyrine (phenazone) after intravenous and oral administration. *Arzneim.-Forsch.* **32**:575–578 (1982).
  43. G. Bouchard, P. A. Carrupt, B. Testa, V. Gobry, and H. H. Girault. Lipophilicity and solvation of anionic drugs. *Chem. Eur. J.* **8**:3478–3484 (2002).
  44. G. Caron, G. Steyaert, A. Pagliara, F. Reymond, P. Crivori, P. Gaillard, P. A. Carrupt, A. Avdeef, J. Comer, K. J. Box, H. H. Girault, and B. Testa. Structure–lipophilicity relationships of neutral and protonated  $\beta$ -blockers. Part I. Intra- and intermolecular effects in isotropic systems. *Helv. Chim. Acta* **82**:1211–1222 (1999).
  45. W. L. Chiou and A. Barve. Linear correlation of the fraction of oral dose absorbed of 64 drugs between humans and rats. *Pharm. Res.* **15**:1792–1795 (1998).
  46. S. M. Nasrallah and F. L. Iber. Mannitol absorption and metabolism in man. *Am. J. Med. Sci.* **258**:80–88 (1969).
  47. F. Ingels, B. Beck, M. Oth, and P. Augustijns. Effect of simulated intestinal fluid on drug permeability estimation across Caco-2 monolayers. *Int. J. Pharm.* **274**:221–232 (2004).
  48. J. Dreyfuss, J. M. Shaw, and J. J. Ross. Absorption of the beta-adrenergic-blocking agent, nadolol, by mice, rats, hamsters, rabbits, dogs, monkeys, and man: an unusual species difference. *Xenobiotica* **8**:503–508 (1978).